Original Article

Direct Effect of Cholesterol on Insulin Secretion

A Novel Mechanism for Pancreatic β-Cell Dysfunction

Mingming Hao, W. Steven Head, Subhadra C. Gunawardana, Alyssa H. Hasty, and David W. Piston

OBJECTIVE—Type 2 diabetes is often accompanied by abnormal blood lipid and lipoprotein levels, but most studies on the link between hyperlipidemia and diabetes have focused on free fatty acids (FFAs). In this study, we examined the relationship between cholesterol and insulin secretion from pancreatic β-cells that is independent of the effects of FFAs.

RESEARCH DESIGN AND METHODS—Several methods were used to modulate cholesterol levels in intact islets and cultured β-cells, including a recently developed mouse model that exhibits elevated cholesterol but normal FFA levels. Acute and metabolic alteration of cholesterol was done using pharmacological reagents.

RESULTS—We found a direct link between elevated serum cholesterol and reduced insulin secretion, with normal secretion restored by cholesterol depletion. We further demonstrate that excess cholesterol inhibits secretion by downregulation of metabolism through increased neuronal nitric oxide synthase dimerization.

CONCLUSIONS—This direct effect of cholesterol on β-cell metabolism opens a novel set of mechanisms that may contribute to β-cell dysfunction and the onset of diabetes in obese patients.
Diabetes **56:2328–2338, 2007**

Diabetes has become a global health problem, affecting >170 million individuals worldwide. The rapid rate of increase in the prevalence of diabetes has profound implications in terms of long-term complications and associated medical costs. Type 2 diabetes accounts for >90% of all cases of diabetes and is characterized by insulin resistance and a defect in insulin secretion from pancreatic β-cells (1). Whereas the relative importance of alterations in insulin sensitivity versus secretion is debatable, it is accepted that hyperglycemia, hence diabetes, does not develop without β-cell dysfunction (2). Alteration of pancreatic β-cell function leading to an impaired insulin secretory response to glucose is hallmark of the transition from the pre-diabetic to the diabetic state (3). Among the many contributing factors, hyperlipidemia plays a critical role in the pathogenesis of β-cell dysfunction (4). The established link between obesity and diabetes, as well as observations that plasma levels of free fatty acids (FFAs) are elevated in most obese individuals, suggests that FFAs might induce hyperglycemia. Lipotoxicity, which refers to the diabetogenic effect of elevated circulating FFAs or cellular fat content, has been studied extensively (5). In addition to FFAs, plasma cholesterol is often elevated in obese patients; yet, the impact of cholesterol in glucose-stimulated insulin secretion (GSIS) from pancreatic β-cells has not been reported.

Cholesterol can regulate signal transduction through membrane microdomains and gene expression through cholesterol-activated transcription factors (6). For example, intracellular cholesterol regulates glucose metabolism and gene expression in adipocytes (7). GSIS is a complex process involving a cascade of regulatory factors. Misregulation of cholesterol could result in disruption of any one pathway and lead to partial or a near complete loss of secretory function. This study focuses on the function of cholesterol-rich membrane microdomains in GSIS.

The plasma membranes of mammalian cells contain 30–50% molar fraction of cholesterol (8). Cholesterol is also enriched in internal membranes (9). Cholesterol plays an essential role in membrane organization, dynamics, and function. It is thought to contribute to the tight packing of lipids by filling interstitial spaces between lipid molecules. Membrane microdomains are small membrane assemblies enriched in cholesterol and sphingolipids and coexist with more fluid domains enriched in phospholipids with unsaturated hydrocarbon chains (10). The formation of these membrane microdomains is seen only within critical concentrations of cholesterol (11). It is well known that both membrane fluidity and curvature are strongly modulated by the amount of cholesterol present in the membrane (12). Membrane microdomains can enhance cell signaling by locally concentrating or excluding selected protein components at specific sites on membranes. In this study, we examine GSIS in β-cells where membrane properties have been altered by depleting or overloading cholesterol.

To date, limited studies on the involvement of membrane microdomains in GSIS from pancreatic β-cells have focused only on proteins at the plasma membrane. It is shown that cholesterol depletion leads to redistribution of K^+ channel $K_V2.1$ and soluble *N*-ethylmaleimide–sensitive factor attachment protein receptor proteins from detergent-resistant to soluble domains in β-cells and in turn

From the Department of Molecular Physiology and Biophysics, Vanderbilt University Medical Center, Nashville, Tennessee.

Address correspondence and reprint requests to David W. Piston, Department of Molecular Physiology and Biophysics, Vanderbilt University Medical Center, 735 Light Hall, Nashville, TN 37232. E-mail: dave.piston@vanderbilt.edu.

Received for publication 15 January 2007 and accepted in revised form 8 June 2007.

Published ahead of print at http://diabetes.diabetesjournals.org on 15 June 2007. DOI: 10.2337/db07-0056.

2-DG, 2-deoxyglucose; apoE, apolipoprotein E; FFA, free fatty acid; GK, glucokinase; GSIS, glucose-stimulated insulin secretion; MβCD, methyl-β-cyclodextrin; nNOS, neuronal nitric oxide synthase.

© 2007 by the American Diabetes Association.

The costs of publication of this article were defrayed in part by the payment of page charges. This article must therefore be hereby marked "advertisement" in accordance with 18 U.S.C. Section 1734 solely to indicate this fact.

Downloaded from http://diabetesjournals.org/diabetes/article-pdf/56/9/2328/388997/zdb00907002328.pdf by guest on 29 June 2022

TABLE 1
Plasma metabolic parameters of mice used in this study

	C57BL/6J	*apoE*$^{-/-}$	*ob/ob*	*ob/ob*;*apoE*$^{-/-}$
n	5	5	5	4
TC (mg/dl)	121.0 ± 31.6	442 ± 65.0*	217 ± 66.6	728.3 ± 156.1†
TG (mg/dl)	51.3 ± 15.6	89.3 ± 14.7‡	107.0 ± 23.1	180.3 ± 36.0§
FFA (mmol/l)	0.49 ± 0.16	0.50 ± 0.11	0.78 ± 0.15	0.86 ± 0.23
Glucose (mg/dl)	125 ± 2.1	113 ± 6.7	118 ± 12‖	132 ± 25‖
Insulin (ng/ml)	0.89 ± 0.19	0.86 ± 0.22	17 ± 3.4‖	31 ± 8.5‖

Data are means ± SD. Six-month-old mice were kept on a standard chow diet. Plasma total cholesterol (TC), triglyceride (TG), and FFA levels were measured using enzymatic methods. Statistical analysis was performed using the Student's *t* test: *$P < 0.01$ vs. C57BL/6J, †$P < 0.01$ vs. *ob/ob*, ‡$P < 0.05$ vs. C57BL/6J, §$P < 0.05$ vs. *ob/ob*. ‖Values were taken from a previously published study (16).

enhances GSIS (13,14). Membrane microdomains also play an essential role in interleukin-1β–induced nitric oxide (NO) release from β-cells (15). Our results in this study show that in addition to changes in proteins present on the plasma membrane, glucose metabolism involving glucokinase (GK) is affected by cholesterol alteration. Here, we show that excess cellular cholesterol is directly linked to reduced GSIS and that normal secretion could be restored by cholesterol depletion. We further demonstrate one potential mechanism for cholesterol regulation of GSIS that involves modification of neuronal NO synthase (nNOS) and GK activity through cholesterol-rich membrane microdomains on the insulin granules.

RESEARCH DESIGN AND METHODS

Mice, cells, and islets. C57BL/6J mice (Harlan Laboratories, Indianapolis, IN) were used, unless otherwise noted. Apolipoprotein E (apoE)-deficient mice (*ApoE*$^{-/-}$) (B6.129P2-*Apoe*^{tm1Unc}/J), matching control mice (C57BL/6J), and nNOS knockout mice (B6.129S4-*Nos1*^{tm1Plh}/J) were purchased from The Jackson Laboratory (Bar Harbor, ME). *ob/ob*;*apoE*$^{-/-}$ mice (on C57BL/6J background) were produced by intercrossing *ob*/+ and *apoE*$^{-/-}$ mice (16). All mice were kept on a rodent chow (LabDiet 5001, 12% of calories from fat) and cared for according to the guidelines of the Vanderbilt Institutional Animal Care and Use Committee. 832/13 INS-1 cells were a kind gift from Dr. Newgard (Duke University, Durham, NC). βTC3 and 832/13 INS-1 insulinoma cells were cultured and prepared for experiments as previously described (17,18). Pancreatic islets were isolated and cultured using methods developed in our lab (19).

Cholesterol assay in islets. Cholesterol content was quantified in a 96-well plate by a fluorometric method using an enzyme-coupled reaction provided by the Amplex Red Cholesterol Assay kit (Molecular Probes). After isolation, islets were divided into two groups for cholesterol and insulin assays. For cholesterol measurement, material from each tube containing 10 islets was subjected to lipid extraction with chloroform/methanol (2:1; vol/vol), dried down to a thin film, and resuspended in 60-μl 1× working solution (Amplex Red Cholesterol Assay kit) supplemented with 0.1% Triton X-100. From that, 50 μl was used for cholesterol assay and 10 μl for protein assay (BCA Protein Assay; Pierce, Rockford, Il).

Glucose-stimulated insulin secretion measurements. Static incubations of pancreatic islets for insulin secretion measurements were done as previously described (19). Insulin radioimmunoassays were performed by the Diabetes Research and Training Center Hormone Core Resource at Vanderbilt University. Mouse serum total cholesterol, triglycerides, and free fatty acids were measured by the Vanderbilt Mouse Metabolic Phenotyping Center Lipid Core.

Cholesterol manipulation. For metabolic depletion, islets were grown for 3 days in metabolic depletion medium (RPMI-1640; similar to the growth medium but with 10% lipoprotein-deficient serum in place of FBS, supplemented with 200 μmol/l mevalonate [required to maintain cell viability] and 10 μmol/l mevastatin) to block cholesterol synthesis and deplete cholesterol stores (20). For depletion by methyl-β-cyclodextrin (MβCD) (Sigma), islets and β-cells were incubated with 10 mmol/l MβCD at 37°C for 1 h, which removed cholesterol from both plasma membrane and intracellular stores because intracellular cholesterol effluxes efficiently to the plasma membrane where it is quickly removed by MβCD as the acceptor (9). To cholesterol overload, cells were incubated with 10 mmol/l soluble cholesterol (Sigma; 1 g contains ~40 mg cholesterol) at 37°C for 1 h.

Glucokinase activity assay. Enzymatic activity of GK was measured by a continuous spectrophotometric rate determination method (21) using 60 mmol/l Tris, 20 mmol/l MgCl, 2.5 mmol/l dithiothreitol, 100 mmol/l KCl, 4 mmol/l adenosine 5′-triphosphate, 0.9 mmol/l β-nicotinamide adenine dinucleotide phosphate, and 10 units glucose 6-phosphate dehydrogenase. One unit of GK activity is defined as phosphorylation of 1 μmol D-glucose to D-glucose 6-phosphate per minute at pH 9.0 at room temperature. GK activity was measured by subtracting the activity measured at 0.5 mmol/l glucose from that at 100 mmol/l glucose to account for hexokinase activity in the cell lysates.

Low-temperature SDS-PAGE. Cells were collected in cold PBS and resuspended in cold lysis buffer (20 mmol/l HEPES, 100 mmol/l NaCl, 1 mmol/l EDTA, 1% cholate, 1% Triton X-100, and 1× protease inhibitor cocktail for mammalian cells [Sigma]). Cold SDS loading buffer (0.05 mol/l Tris-HCl, pH 6.8, 2% SDS, 10% glycerol, 100 mmol/l dithiothreitol, and 0.1% bromphenol blue) was added to the cell lysate and incubated for 5 min at 0°C. Samples were loaded on 6% polyacrylamide gels, subjected to electrophoresis at 0°C, and visualized by immunoblotting with nNOS monoclonal antibody (BD Transduction Laboratories) and peroxidase-conjugated secondary antibody. To separate the cytoplasmic and membrane-bound fractions, digitonin permeabilization was performed as described previously (22), with the exception of using 10 μg/ml instead of 20 μg/ml digitonin.

Statistical analysis. Results are expressed as means ± SD. Unpaired two-tailed Student's *t* tests were performed for comparisons between treated and control groups. Differences were considered significant at $P < 0.05$. In cholesterol and insulin secretion assays, *n* denotes the number of mice used for each condition. Samples of 10 islets each were taken from each mouse. In all other experiments using cultured β-cells, *n* denotes the number of times each experiment was repeated with different plates of cells for each condition.

RESULTS

GSIS is directly affected by islet cholesterol levels. Traditionally, a high-fat diet is used to increase serum cholesterol levels in mice. However, this is also accompanied by elevations in FFA levels. To circumvent this issue, we used apoE-deficient (*apoE*$^{-/-}$) mice fed a standard diet. Compared with control C57BL/6J animals, *apoE*$^{-/-}$ mice have elevated plasma cholesterol levels without changes in plasma FFA. Furthermore, when the *apoE*$^{-/-}$ mice are made obese by placing them on a leptin-deficient *ob/ob* background, plasma cholesterol levels are further elevated, again without concomitant increases in FFA compared with *ob/ob* controls (Table 1). Because apoE is not present in the pancreatic islets of wild-type mice (23), its absence does not directly affect islet function when studied in vitro, and we observed similar islet morphology between *apoE*$^{-/-}$ and control mice (*apoE*$^{-/-}$ vs. C57BL/6J and *ob/ob*;*apoE*$^{-/-}$ vs. *ob/ob*). Cholesterol measurements in pancreatic islets show that an increase in serum cholesterol (Table 1) leads to increased islet cholesterol (Fig. 1*A*). Although total insulin content does not vary significantly among different mouse models (Fig. 1*B*), the increase in islet cholesterol causes a dramatic reduction in the islets' ability to secrete insulin in response to basal and high glucose concentrations (Fig. 1*C*). This result indicates

Downloaded from http://diabetesjournals.org/diabetes/article-pdf/56/9/2328/388997/zdb00907002328.pdf by guest on 29 June 2022

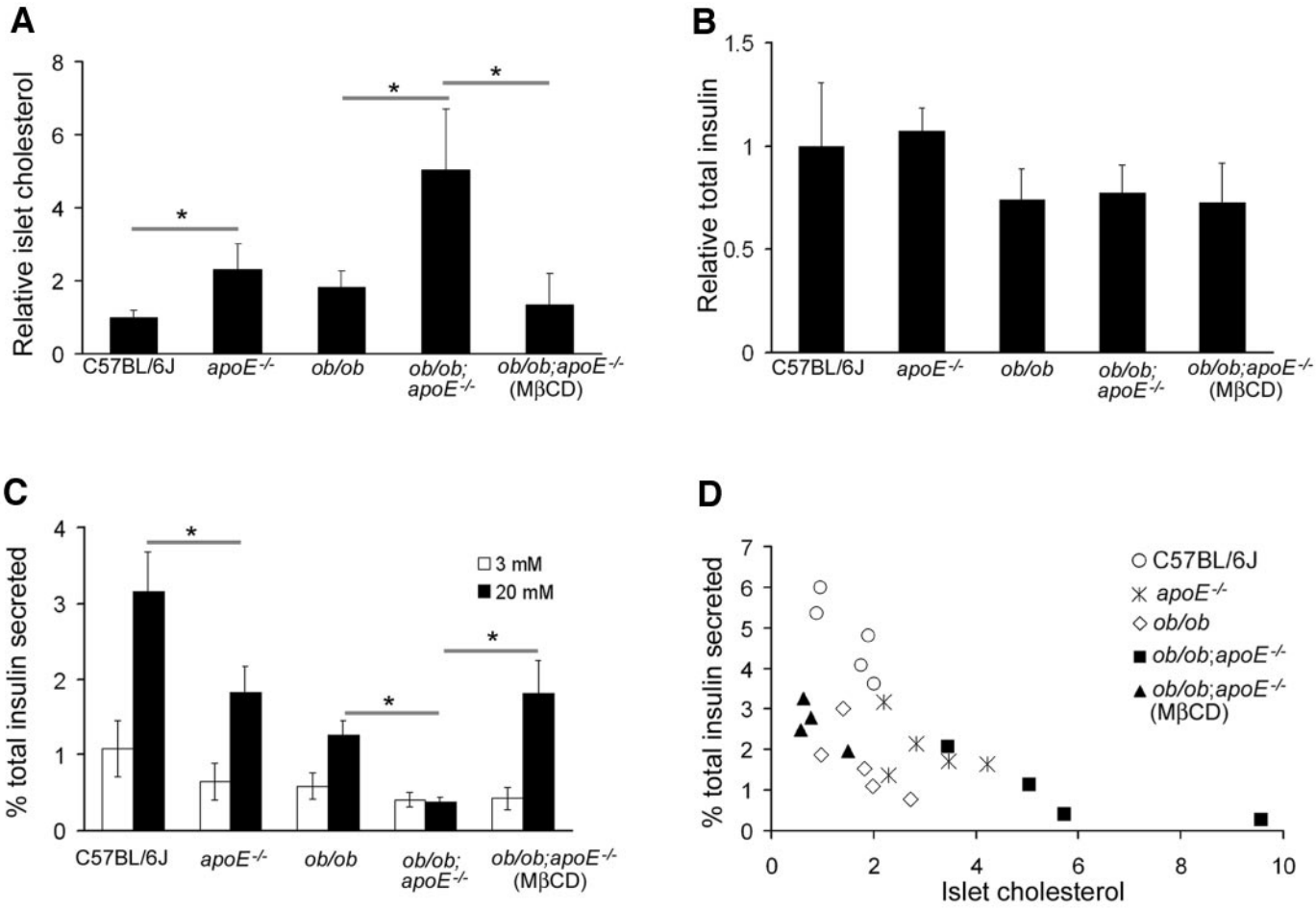

FIG. 1. Reduced GSIS from pancreatic islets in mice with elevated cholesterol levels. Islets were isolated from four mouse strains, as indicated, and the number of mice used from each strain is listed in Table 1. Each sample consisted of 10 islets, and the results were taken from an average of triplicate samples. For results, labeled *ob/ob;apoE*$^{-/-}$(MβCD) islets from *ob/ob;apoE*$^{-/-}$ mice were incubated with 10 mmol/l MβCD for 1 h shaking at 37°C before taking measurements. GSIS was measured using static incubations of isolated islets: islets were first incubated in 2 mmol/l glucose for 1 h before transferred to different concentrations of glucose. At the end of the 1-h stimulation period, samples were collected for insulin measurement followed by the addition of 1% Triton X-100 to determine total insulin content. *A*: Islet cholesterol levels were determined from lipids extracted from each sample and normalized to the protein content in the same sample, *$P < 0.05$. *B*: Total islet insulin levels were measured from Triton X-100–extracted samples and normalized to the protein content in the same sample. *C*: Insulin secretion in response to 3 and 20 mmol/l glucose from each sample, expressed as fractional release, *$P < 0.05$. *D*: GSIS (20 mmol/l glucose) plotted against islet cholesterol levels. Each data point represents an average of triplicate samples from one mouse.

that cholesterol directly impacts GSIS independent of the cellular FFA content.

Because plasma triglyceride levels are also elevated in our mouse models relative to their respective controls (Table 1), we studied isolated islets in which cholesterol can be specifically manipulated. To determine whether direct cholesterol depletion could enhance GSIS from isolated C57BL/6J islets, MβCD was used for 1 h to cause acute depletion of cellular cholesterol (9) and mevastatin (a cholesterol biosynthesis inhibitor) to cause metabolic depletion over several days in culture (20). With these treatments, islet cholesterol was reduced by 30–40% (Fig. 2*A*), whereas total insulin content remained unaffected (Fig. 2*B*). Direct cholesterol depletion from isolated islets significantly enhances insulin secretion under both basal and high glucose concentrations (Fig. 2*C*). Cholesterol depletion of the *ob/ob;apoE*$^{-/-}$ islets using MβCD also partially restores GSIS (Fig. 1*C*). GSIS (20 mmol/l glucose) is shown as a function of islet cholesterol for the genetically modified mouse models (Fig. 1*D*) or isolated wild-type islets with different cholesterol levels (Fig. 2*D*). Although many factors affect insulin secretion, in all of these cases, the islet cholesterol level is inversely correlated to β-cell GSIS.

Glucose metabolism is involved in cholesterol-regulated GSIS from β-cells. To investigate the molecular mechanisms underlying cholesterol-dependent GSIS, we turned to cultured pancreatic β-cells. Both 832/13 INS-1 and βTC3 cells secrete insulin in a regulated manner (18,24). INS-1 cells are used for the functional experiments because of their robust responsiveness to glucose (18), and βTC3 cells are used for the imaging experiments because of their low autofluorescence. The capability to manipulate cholesterol in these insulinoma cells is greatly improved relative to that in islets, so that cholesterol overloading using soluble cholesterol (cholesterol loaded on MβCD) is possible (Fig. 3*A*). In INS-1 cells, using MβCD to deplete cholesterol before glucose stimulation increases insulin secretion at all tested glucose concentrations (Fig. 3*B*). In contrast, cholesterol overload suppresses GSIS (Fig. 3*B*). Similar results are observed in βTC3 cells for changes in intracellular Ca^{2+}, a critical signaling molecule in GSIS (Fig. 3*C*). The increase in intracellular Ca^{2+} on glucose stimulation is reduced in

Downloaded from http://diabetesjournals.org/diabetes/article-pdf/56/9/2328/388997/zdb00907002328.pdf by guest on 29 June 2022

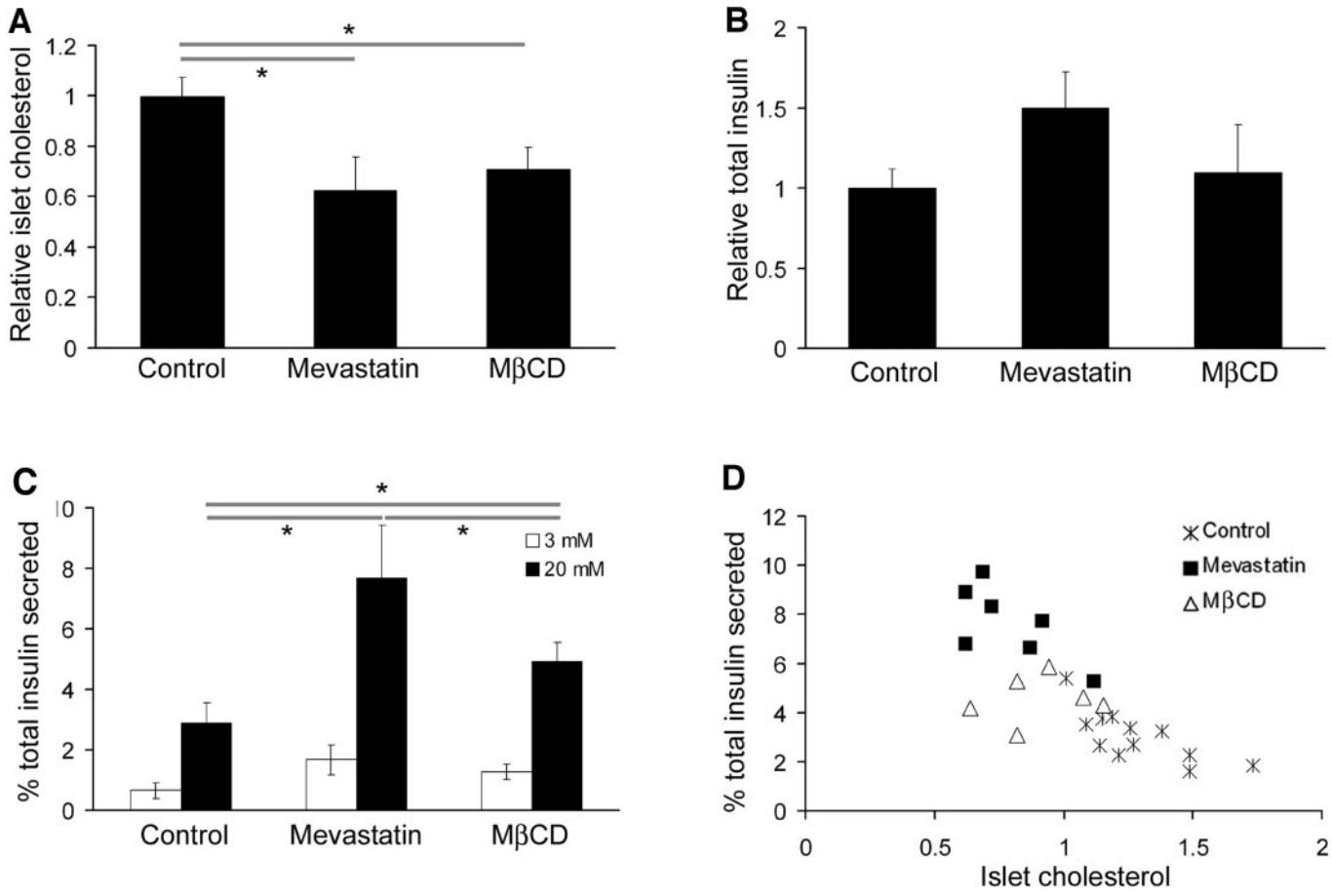

FIG. 2. Enhanced GSIS from wild-type pancreatic islets with reduced cholesterol levels. Two methods of cholesterol depletion were used on islets isolated from C57BL/6J: acute depletion by MβCD (n = 6) and metabolic depletion by mevastatin (n = 7). n = 12 mice for control islets. Each sample consisted of 10 islets, and the results were taken from an average of triplicate samples. GSIS was measured using the method described in Fig. 1. *A*: Islet cholesterol levels were determined from lipids extracted from each sample and normalized to the protein content in the same sample, *$P < 0.05$. *B*: Total islet insulin levels were measured from Triton X-100–extracted samples and normalized to the protein content in the same sample. *C*: Insulin secretion in response to 3 and 20 mmol/l glucose from each sample, expressed as fractional release, *$P < 0.05$. *D*: GSIS (20 mmol/l glucose) plotted against islet cholesterol levels. Each data point represents an average of triplicate samples from one mouse.

islets from *ob/ob*;*apoE*$^{-/-}$ versus *ob/ob* mice (Fig. 3*D*). To determine whether cholesterol depletion alone is sufficient to stimulate insulin secretion, we used a fluorescent zinc indicator (FluoZin-3) to monitor insulin release from MβCD-treated βTC3 cells. FluoZin-3 has been successfully used to study insulin release in pancreatic β-cells because insulin and Zn^{2+} are co-released by exocytosis (25). When 10 mmol/l MβCD is added to βTC3 cells kept in 2 mmol/l glucose, a rise in FluoZin-3 fluorescence indicates the initiation of insulin secretion after cholesterol removal, even in the absence of other insulin secretagogues (Fig. 3*E*).

Because cholesterol directly affects GSIS, we examined the glucose-stimulated signal transduction pathway to see where cholesterol action occurs. To determine whether cholesterol is coupled to proximal glucose metabolism, we monitored the effect of MβCD treatment on intracellular Ca^{2+} in the presence or absence of a nonmetabolizable glucose analog, 2-deoxyglucose (2-DG). As shown in Fig. 3*F*, adding MβCD to βTC3 cells in 2 mmol/l glucose raises intracellular Ca^{2+}. However, the increase in intracellular Ca^{2+} caused by cholesterol depletion is blunted when glucose is replaced by 2-DG, suggesting that glucose metabolism is required for initiating insulin secretory response in cholesterol-depleted cells. We also used NADPH autofluorescence to assay cellular redox state (26). Pretreating βTC3 cells with MβCD leads to a slightly higher NADPH production on 20 mmol/l glucose stimulation compared with the control cells (Fig. 4*A*). Overloading with cholesterol before glucose stimulation decreases NADPH production (Fig. 4*A*). Compared with *ob/ob* mice, NADPH production in islets from *ob/ob*;*apoE*$^{-/-}$ mice is significantly reduced (Fig. 4*B*). As with Zn^{2+} secretion (Fig. 3*E*) and intracellular Ca^{2+} (Fig. 3*F*), cholesterol depletion with MβCD alone initiates NADPH production (Fig. 4*C*). NADPH fluorescence does not increase in response to MβCD when 2-DG is present or when soluble cholesterol is added to the cells (Fig. 4*D*). These results suggest that the effect of cholesterol depletion using MβCD on intracellular Ca^{2+} increase, NADPH production, and insulin secretion (indicated by Zn^{2+} release) involves proximal glucose metabolism.

Cholesterol is involved in nNOS regulation of GK. GK critically regulates GSIS by exerting tight control over glucose metabolism. Its unique glucose-sensing property underlies the ability of pancreatic β-cells to respond to plasma glucose fluctuations. Because of this, even small changes in GK activity have an impact on the rate of GSIS (27). This is supported by many studies of inactivating mutations in the gene encoding GK in humans with

Downloaded from http://diabetesjournals.org/diabetes/article-pdf/56/9/2328/388997/zdb00907002328.pdf by guest on 29 June 2022

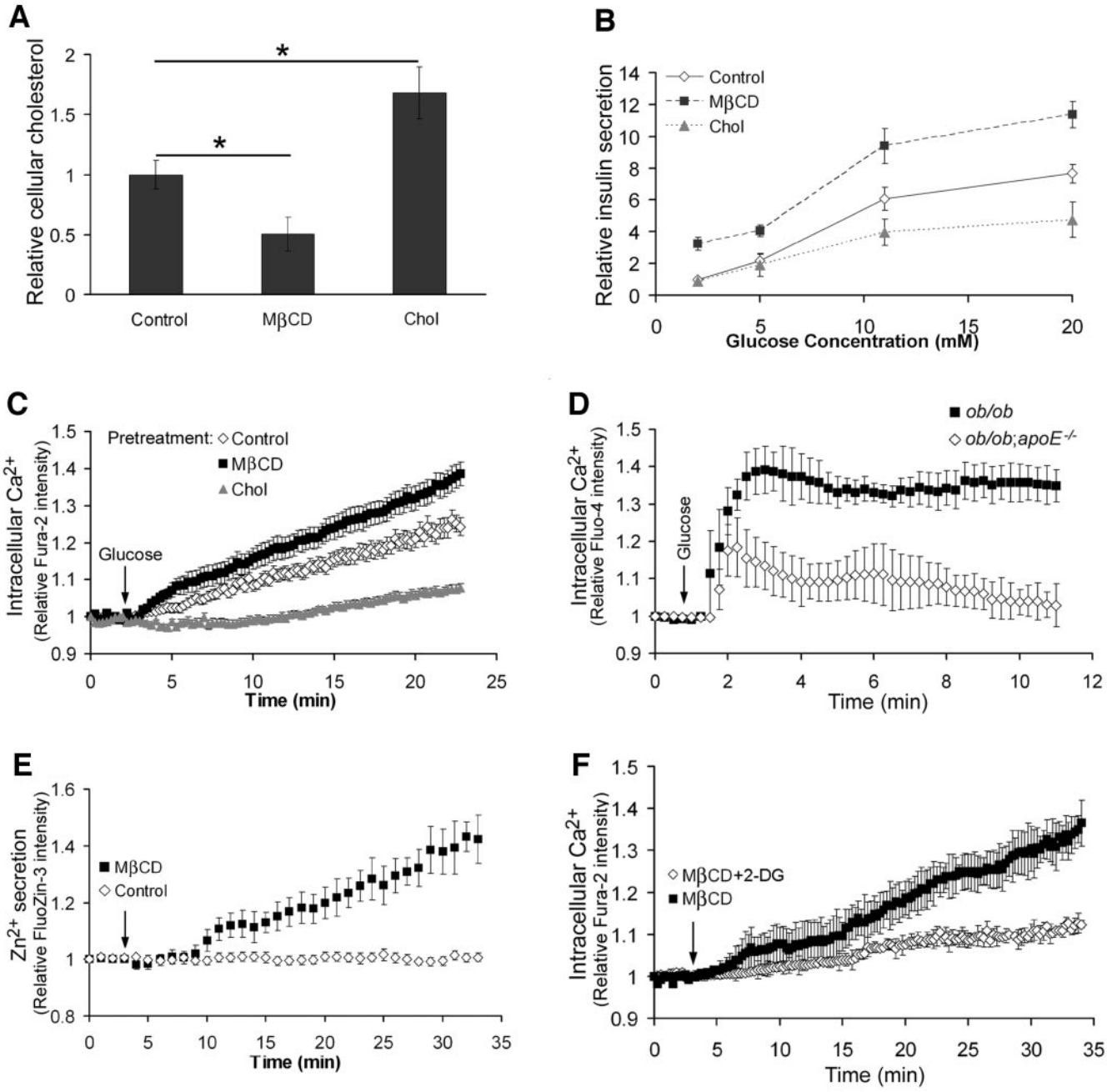

FIG. 3. Cellular cholesterol levels affect GSIS from cultured pancreatic β-cells. Cholesterol depletion and overloading in cultured β-cells were done using 10 mmol/l MβCD and 10 mmol/l soluble cholesterol (Chol), respectively, for 1 h at 37°C before taking measurements. *A* and *B*: Cellular cholesterol levels and GSIS, respectively, in 832/13 INS-1 cells after cholesterol treatment. GSIS was measured using the method described in Fig. 1 from cells plated in 12-well plates. *A*: $n = 8$, *$P < 0.05$. *B*: $n = 5$, $P < 0.01$ between MβCD-treated and control cells for all glucose concentrations; $P < 0.05$ between cholesterol-treated and control cells for 11 and 20 mmol/l glucose. *C*: Glucose-stimulated intracellular Ca^{2+} response of βTC3 cells with different levels of cellular cholesterol. Cells kept in glucose-free buffer underwent cholesterol treatment before loading with 2 μmol/l Fura-2. A 340- to 380-nm intensity ratio of Fura-2 was obtained from the entire image after background correction. The arrow points to when 20 mmol/l glucose was added. $n = 6$, $P < 0.05$ between MβCD-treated and control cells and $P < 0.01$ between cholesterol-treated and control cells for all time points 3 min postglucose addition. *D*: Glucose-stimulated intracellular Ca^{2+} response of islets from *ob/ob* and *ob/ob;apoE*$^{-/-}$ mice. Cultured islets were labeled with 4 μmol/l Fluo-4 in 2 mmol/l glucose at room temperature for 1 h. The arrow indicates when 20 mmol/l glucose was added. $n = 5$, $P < 0.01$ for all time points 2 min after glucose addition. *E*: Time course detection of Zn^{2+} secretion in MβCD-treated βTC3 cells. Images were taken in the presence of FluoZin-3 added to the extracellular medium of cells kept in 2 mmol/l glucose. Fluorescence quantification was done on three small regions in the extracellular medium, as determined by the differential interference contrast image. The arrow indicates the addition of buffer (control) or MβCD (10 mmol/l final concentration). $n = 7$, $P < 0.01$ for all time points 11 min after the start of the experiment. *F*: Changes in intracellular Ca^{2+} in response to MβCD with and without a nonmetabolizable glucose analog (2-DG). Fura-2–loaded βTC3 cells were kept in either 2 mmol/l glucose or 5 mmol/l 2-DG throughout. The arrow indicates the addition of MβCD. $n = 6$, $P < 0.01$ for all time points 15 min after the start of the experiment.

maturity-onset diabetes of the young (28). It has been shown on glucose stimulation that GK dissociates from the insulin granules and is released to the cytoplasm, where it is activated (29), as depicted in Fig. 5*A*. In this study, pretreating INS-1 cells with MβCD enhances GK activity under both basal (3 mmol/l) and high glucose (20 mmol/l) concentrations (Fig. 5*B*). In contrast, cholesterol overloading decreases GK activity on glucose stimulation (Fig. 5*B*).

Downloaded from http://diabetesjournals.org/diabetes/article-pdf/56/9/2328/388997/zdb00907002328.pdf by guest on 29 June 2022

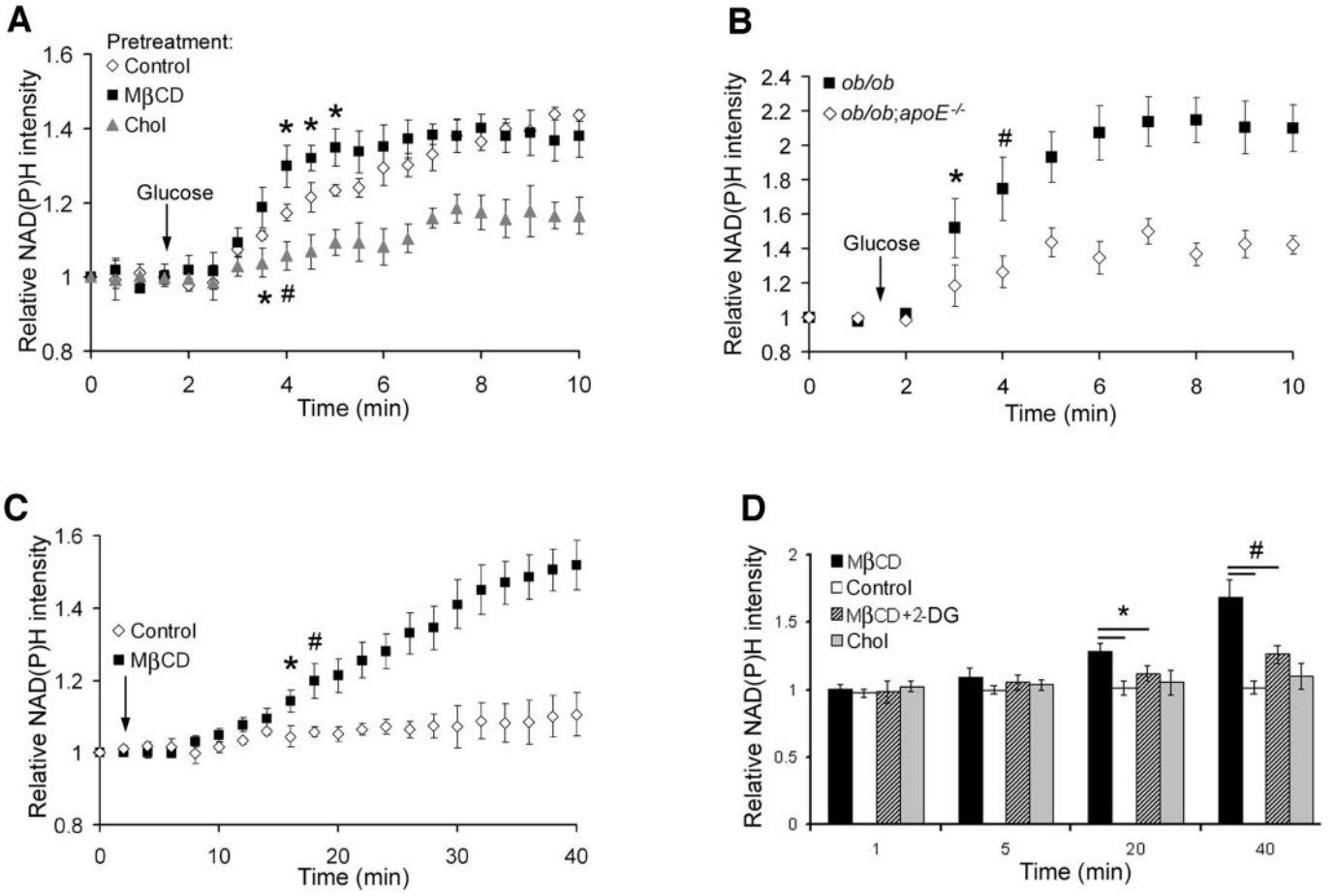

FIG. 4. Cholesterol-dependent regulation of GSIS involves glucose metabolism. *A*: Time-course imaging of NADPH response of βTC3 cells stimulated with 20 mmol/l glucose. Glucose-starved cells underwent cholesterol treatment before NADPH imaging (40× Plan Neofluar 1.3 NA objective lens, 710-nm mode-locked Ti:Saph laser and a nondescanned detector with a custom 380- to 550-nm filter). The arrow indicates the addition of 20 mmol/l glucose. $n = 5$, *$P < 0.05$ vs. control. #$P < 0.01$ vs. control for this and all subsequent time points. *B*: NADPH response of islets from *ob/ob* and *ob/ob;apoE*$^{-/-}$ mice. Cultured islets were incubated in 2 mmol/l glucose for 1 h before imaging. The arrow indicates the addition of 20 mmol/l glucose. $n = 5$, *$P < 0.05$ and #$P < 0.01$ for this and all subsequent time points. *C*: NADPH response to MβCD treatment in βTC3 cells kept in 2 mmol/l glucose. The arrow indicates the addition of buffer (control) or MβCD (10 mmol/l final concentration). $n = 7$, *$P < 0.05$ and #$P < 0.01$ for this and all subsequent time points. *D*: NADPH response in βTC3 cells kept in 2 mmol/l glucose or 5 mmol/l 2-DG and subjected to different cholesterol treatments. The X-axis shows the time elapsed since the addition of indicated reagents. $n = 5$, *$P < 0.05$ and #$P < 0.01$.

We next examined GK translocation by immunoblotting of the pellet (membrane) and soluble (cytoplasmic) fractions of digitonin-permeabilized cells under different conditions. Translocation of GK from the membrane bound to the cytoplasmic fraction is observed on cholesterol depletion (Fig. 5*C*). Further, glucose stimulation results in an additional increase in GK activity and translocation in MβCD-treated cells (Fig. 5*B* and *C*), which may suggest that cholesterol depletion and glucose stimulation utilize separate mechanisms for GK regulation.

Previous evidence indicates that glucose-stimulated GK translocation involves S-nitrosylation of by nNOS (29). To determine whether nNOS activity impacts GK in cholesterol-depleted cells, we examined nNOS activity using a fluorescent NO indicator, DAF-FM (4-amino-5-methylamino-2′,7′-difluorofluorescein). Figure 6*A* shows that cholesterol depletion before insulin stimulation prevents NO production observed in control cells. Insulin was used here as the stimulant because it caused a more rapid change in nNOS activity than glucose (29). The inhibition in NO production is consistent with the observation that disruption of lipid microdomains by MβCD results in reduced NO release from insulin-secreting cells (15). Adding MβCD to βTC3 cells in 2 mmol/l glucose leads to a decrease in DAF-FM fluorescence, indicating that cellular NO content is reduced on cholesterol depletion (Fig. 6*B*). These results suggest that nNOS activity is inhibited by cholesterol depletion.

Since cholesterol modulation using MβCD occurs within 30 min (30), its effect on nNOS and GK activity is unlikely to work through changes in gene transcription or protein stability. To determine how cholesterol depletion might decrease nNOS activity and release GK from insulin granules, we looked at the role of cholesterol-rich membrane microdomains in determining nNOS properties. nNOS is localized to insulin granules through its interaction with the transmembrane protein insolinoma-associated protein 2 in pancreatic β-cells (31). Characterization of nNOS has shown that the native protein is a homodimer (32), and dimerization is absolutely required for nNOS activity (33). Thus, we hypothesized a model where cholesterol depletion disrupts nNOS dimers, which in turn weakens the association between nNOS and GK, thereby releasing GK to the cytoplasms, where it becomes activated. Excess cholesterol, on the other hand, stabilizes nNOS dimers and

Downloaded from http://diabetesjournals.org/diabetes/article-pdf/56/9/2328/388997/zdb00907002328.pdf by guest on 29 June 2022

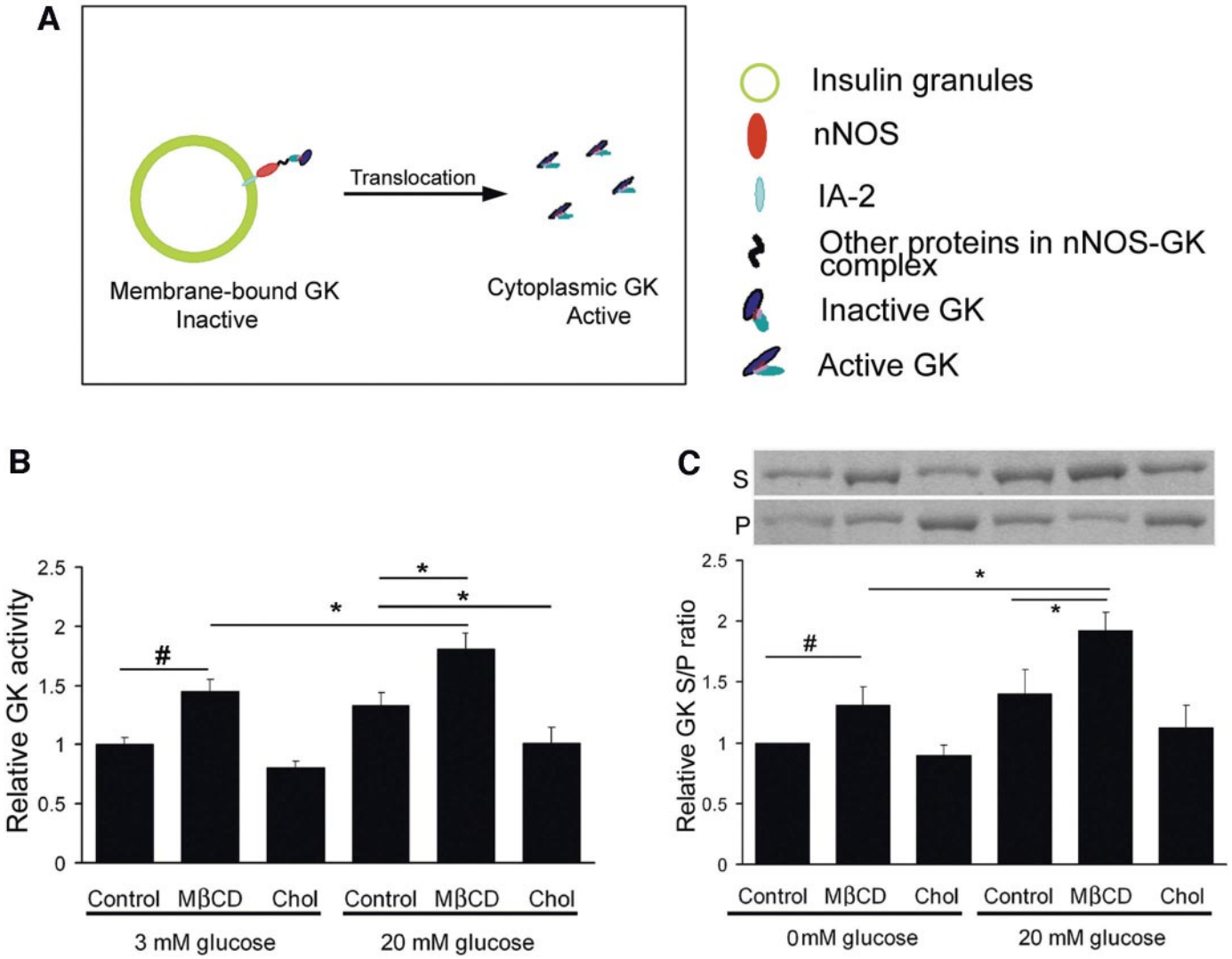

FIG. 5. Cholesterol modulation changes GK activity and localization. *A*: Schematic drawing of how GK activity is related to its cellular localization (see ref. 29). Glucose stimulation results in translocation of GK from insulin granules to the cytoplasm where GK is activated. *B*: GK enzymatic activity in 832/13 INS-1 cells under different conditions and normalized to that measured in control cells under basal glucose. $n = 8$, *$P < 0.05$ and #$P < 0.01$. *C*: Translocation of GK from the membrane-bound to the cytoplasmic fraction in 832/13 INS-1 cells under different conditions. Distribution of GK was quantified by taking a ratio of the amount of GK present in the digitonin-soluble (S, cytoplasmic) fraction to that in the pellet (P, membrane-bound) fraction, and normalized to that in glucose-starved control cells. $n = 6$, *$P < 0.05$ and #$P < 0.01$.

keeps GK bound to insulin granules, where it is less active (Fig. 6*C*).

To test this hypothesis, we immunoprecipitated nNOS from cell lysates and probed by immunoblot for GK. As shown in Fig. 7*A*, cholesterol depletion by MβCD treatment results in dissociation of GK from nNOS under both low and high glucose. In contrast, cholesterol overloading increases association of GK with nNOS on glucose stimulation. There is an additional weakening of the interaction between GK and nNOS when MβCD-treated cells are stimulated with high glucose (Fig. 7*A*), again possibly suggesting that nNOS regulation of GK by cholesterol depletion is different from that by glucose stimulation. Our hypothesis is further supported by the fact that GSIS is greatly enhanced in nNOS knockout mice (Fig. 7*B*), consistent with the idea that a weaker association of GK with insulin granules (due to the lack of granule-associated nNOS) leads to greater GK activity in β-cells. Using low-temperature SDS-PAGE (34), we show that there is less nNOS dimerization in cholesterol-depleted cells compared with untreated cells and that the opposite is observed with cholesterol overloading (Fig. 7*C*). We also measured the nNOS dimer and monomer distribution in the membrane-bound and cytoplasmic fractions using digitonin permeabilization. In both control and cholesterol-depleted cells, there are more nNOS dimers in the pellet fraction, suggesting that the dimer structure is enriched in the insulin granule membranes (Fig. 7*D*). Furthermore, the nNOS oligomeric state dramatically shifts from predominately dimers to mostly monomers in the membrane-bound fraction on cholesterol depletion. These results show that cholesterol depletion disrupts nNOS dimers associated with insulin granules and leads to decreased nNOS activity (Fig. 6*A* and *B*). This is consistent with the previous finding that disruption of the dimeric state of nNOS by its inhibitors affects the secretagogue-induced insulin response (35). Although the exact mechanism by which nNOS dimerization is affected by membrane structure remains unknown, it is conceivable that clustering of insolinoma-associated protein 2 in cholesterol-rich do-

Downloaded from http://diabetesjournals.org/diabetes/article-pdf/56/9/2328/388997/zdb00907002328.pdf by guest on 29 June 2022

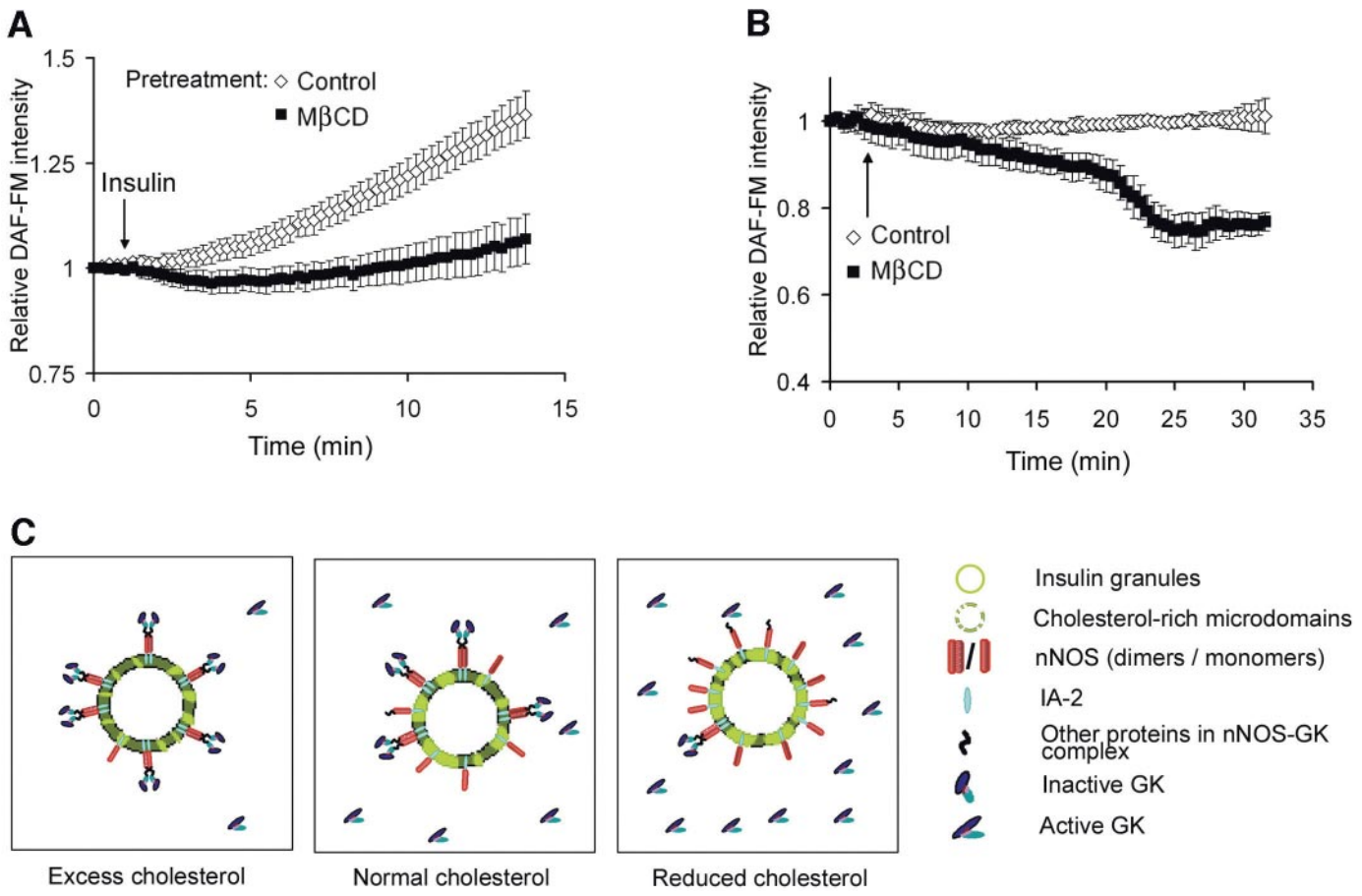

FIG. 6. Cholesterol depletion inhibits nNOS activity. *A*: Reduced NO production in insulin-stimulated βTC3 cells pretreated with MβCD, detected using a fluorescent indicator (DAF-FM). The arrow indicates the addition of 100 nmol/l insulin. $n = 5$. *B*: Decreased cellular NO content in response to MβCD. βTC3 cells were kept in 2 mmol/l glucose and loaded with DAF-FM. The arrow indicates the addition of buffer (control) or MβCD (10 mmol/l final concentration). $n = 5$. *C*: Proposed model of nNOS regulation of GK by its dimeric state at different cholesterol levels. Cholesterol depletion disrupts nNOS dimers and weakens the association between nNOS and GK, leading to the release of GK to the cytoplasm, where it is activated. Excess cholesterol stabilizes nNOS dimers and keeps GK bound to insulin granules, where it is less active.

mains effectively increases the local concentration of nNOS, thus promoting dimer formation.

DISCUSSION

Our results indicate that excess cellular cholesterol plays a direct role in pancreatic islet dysfunction and may well be a key factor underlying the progression of type 2 diabetes. Using different animal models, we show that elevated serum cholesterol leads to increased cholesterol in pancreatic islets. More importantly, islet cholesterol levels directly and significantly impact the extent of GSIS, independent of FFA levels. This has great implications because it indicates the existence of a novel mechanism linking hyperlipidemia and the pathogenesis of type 2 diabetes that is independent of FFAs. It also suggests that the regulation of cellular cholesterol may be a potential target for therapeutic intervention aimed at preserving or improving GSIS function in pancreatic β-cells.

It has been shown that VLDL is markedly increased in *apoE*$^{-/-}$ mice (36), and VLDL exposure leads to a decrease in insulin mRNA levels in βTC3 cells (37). However, we did not find a significant difference between control and *apoE*$^{-/-}$ mice in either plasma insulin levels (Table 1) or total islet insulin content (Fig. 1*B*). The discrepancy might be due to the difference in the cells used (cultured insulinoma cells vs. islets), cholesterol-to-triglyceride ratio of the VLDL particles (triglyceride-rich human VLDL vs. triglyceride-poor *apoE*$^{-/-}$ VLDL), or the length of exposure time (short term vs. chronic). ApoE deficiency is shown to induce greater insulin sensitivity (38). This may explain the relatively normal glucose tolerance in *apoE*$^{-/-}$ mice despite the reduced GSIS observed in our study.

Because of the profound effects of cholesterol on lipid organization and cellular functions, cells have formulated comprehensive mechanisms to maintain membrane cholesterol levels within a narrow range (39). Among all the signal transduction pathways in which cholesterol may be involved in β-cells, we have focused on the role of cholesterol-rich membrane domains in GSIS and one molecular mechanism in particular involving nNOS regulation of GK. Our data show that cholesterol depletion results in a change of nNOS dimer-to-monomer ratio, which in turn causes translocation of GK from insulin granules to the cytoplasm, where it is activated. In contrast, excess cholesterol prevents GK activation by keeping GK bound to insulin granules. Further studies are underway to provide additional details for other GSIS pathways that may also be affected by cholesterol modulation.

Membrane microdomains have raised great interest because they are proposed to be involved in many cellular functions, including signal transduction, protein trafficking, and cell polarization, as well as pathogenesis of many diseases (40). Cholesterol is an essential component of many putative membrane domains, and removal of choles-

Downloaded from http://diabetesjournals.org/diabetes/article-pdf/56/9/2328/388997/zdb00907002328.pdf by guest on 29 June 2022

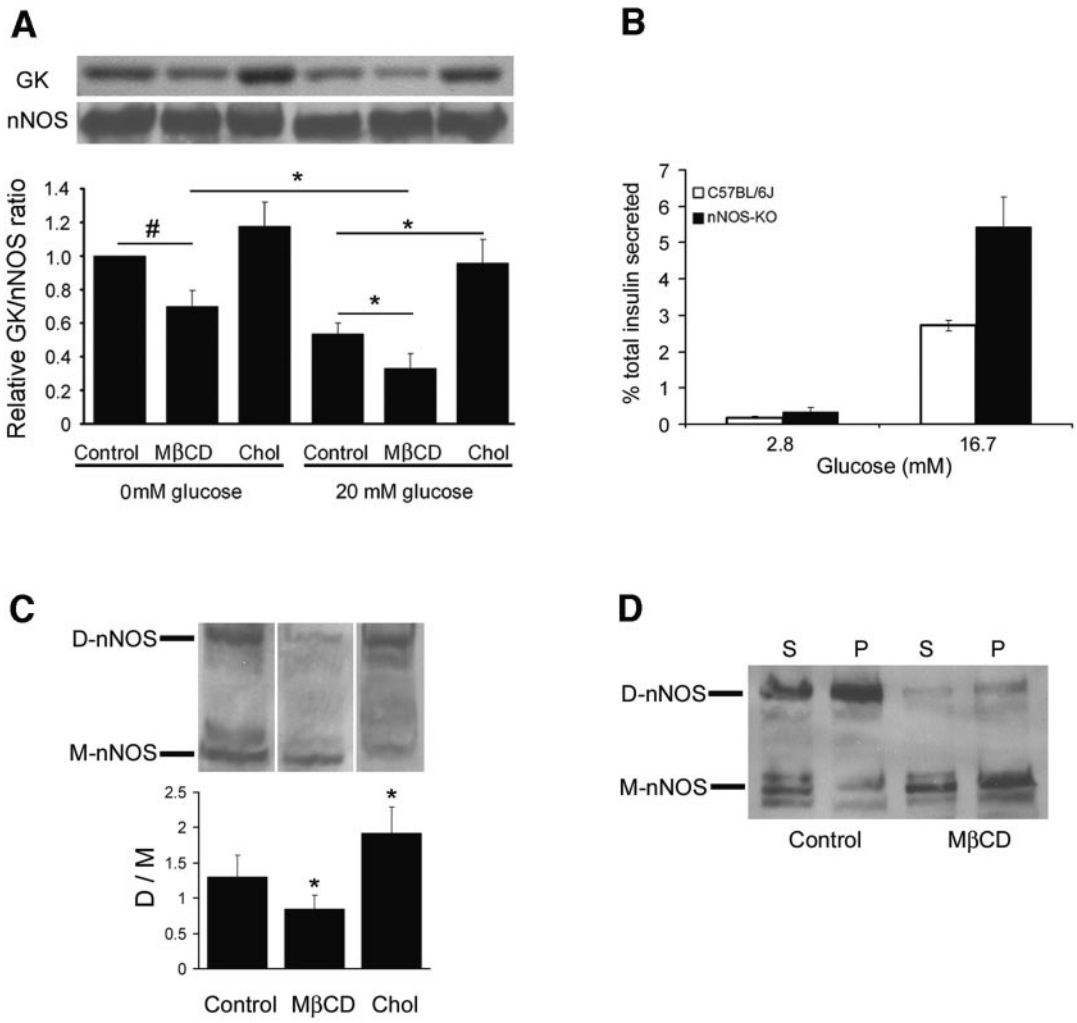

FIG. 7. Cellular cholesterol levels affect the interaction between GK and nNOS through altering nNOS dimeric state. *A*: Association of GK with nNOS in 832/13 INS-1 cells under different conditions. Pellets immunoprecipitated from cell lysates using anti-nNOS preconjugated to Sepharose beads were analyzed by immunoblot using anti-nNOS and anti-GK antibodies. GK association with nNOS was quantified by taking the ratio of GK to nNOS signal and expressed as fraction of that in glucose-starved control cells. $n = 6$. *$P < 0.05$ and #$P > 0.01$. *B*: GSIS from islets isolated from nNOS knockout (nNOS-KO) mice. GSIS was measured using the method described in Fig. 1. $n = 7$. *C*: Detection of nNOS dimers (D-nNOS) and monomers (M-nNOS) in control, cholesterol-depleted (MβCD), and overloaded (Chol) 832/13 INS-1 cells using low-temperature SDS-PAGE. $n = 5$. *$P < 0.05$ vs. control. *D*: Detection of nNOS dimers and monomers in control and cholesterol-depleted 832/13 INS-1 cells permeabilized by digitonin. Pellet (P, membrane-bound) and soluble (S, cytoplasmic) fractions were analyzed by low-temperature SDS-PAGE.

terol disrupts the function of proteins residing in these domains. It has been shown that MβCD treatment results in enhanced GSIS from HIT-T15 hamster insulinoma cells, due to redistribution of voltage-gated K^+ channel and soluble *N*-ethylmaleimide–sensitive factor attachment protein receptor proteins of the putative membrane microdomains (13). However, our results indicate that glucose metabolism is directly affected by cholesterol depletion in addition to any changes in plasma membrane protein distribution that may occur. Our data also suggest that the function of two proteins critically involved in GSIS, nNOS, and GK depends on the cholesterol-enriched lipid environment of insulin granules. nNOS is found to be associated with granule membranes in many cell types. In neurons, MβCD redistributes nNOS from the Triton X-100 insoluble to the soluble fraction, and cholesterol repletion reverses nNOS localization (41). Several lines of evidence have shown that some intracellular membranes not only contain high amounts of cholesterol but also form detergent insoluble domains (42). For example, cholesterol makes up ~70% of the lipids in bovine pituitary secretory granule membranes (43). Cholesterol offers the rigidity necessary for membrane curvature during secretory granule biogenesis. Insulin is packaged into dense core granules, which bud from the *trans*-Golgi network containing cholesterol and sphingolipid-rich microdomains (44).

Although the relationship between elevated cholesterol and diabetes has not been extensively examined, there is some evidence supporting a potential link between the two. First, a locus on chromosome 9 is associated with both the control of cholesterol levels and diabetes (45). Second, blood lipoprotein levels are an indication of the plasma cholesterol content and have been confirmed as important predictors for the onset of type 2 diabetes (46). In a recent study (46) aimed at examining the link between the use of a statin, which lowers serum cholesterol concentration, and subsequent risk of developing diabetes, it was shown that preventative administration of pravastatin reduced the occurrence of type 2 diabetes by 30%. However, results from this type of study are thus far inconclusive. Even though obesity has been identified as an important risk factor for type 2 diabetes, only a small

Downloaded from http://diabetesjournals.org/diabetes/article-pdf/56/9/2328/388997/zdb00907002328.pdf by guest on 29 June 2022

percentage of obese patients will eventually develop the disease. Research suggests that predisposition to the development of type 2 diabetes may be due to genetic differences, although the specific genes involved have not yet been identified. Type 2 diabetes has been associated with high synthesis and low absorption of cholesterol, indicating a link between glucose and cholesterol metabolism (47–50). Indeed, our study opens the possibility that genetic variations relating to cellular cholesterol management may play a role in this genetic predisposition for type 2 diabetes.

ACKNOWLEDGMENTS

This work is supported by grants from the National Institutes of Health (DK67821 to S.C.G., DK53434 to D.W.P., U24-DK59637 to the Metabolic Phenotyping Center, and DK-20593 to the Vanderbilt Diabetes Training and Research Center), the American Heart Association (0330011N to A.H.H.), and the American Diabetes Association (1-04-JF-20 to A.H.H.).

We thank Dr. Kevin D. Niswender for helpful discussions and Drs. Dick Goodman, Britton Chance, Roland Stein, Owen McGuinness, Al Beth, and Alan Cherrington for critical reading of the manuscript.

REFERENCES

1. Yki-Jarvinen H: Pathogenesis of non-insulin-dependent diabetes mellitus. *Lancet* 343:91–95, 1994
2. Kahn SE: The relative contributions of insulin resistance and beta-cell dysfunction to the pathophysiology of type 2 diabetes. *Diabetologia* 46:3–19, 2003
3. Lyssenko V, Almgren P, Anevski D, Perfekt R, Lahti K, Nissen M, Isomaa B, Forsen B, Homstrom N, Saloranta C, Taskinen MR, Groop L, Tuomi T: Predictors of and longitudinal changes in insulin sensitivity and secretion preceding onset of type 2 diabetes. *Diabetes* 54:166–174, 2005
4. Unger RH: Lipotoxicity in the pathogenesis of obesity-dependent NIDDM: genetic and clinical implications. *Diabetes* 44:863–870, 1995
5. Yaney GC, Corkey BE: Fatty acid metabolism and insulin secretion in pancreatic beta cells. *Diabetologia* 46:1297–1312, 2003
6. Brown MS, Goldstein JL: The SREBP pathway: regulation of cholesterol metabolism by proteolysis of a membrane-bound transcription factor. *Cell* 89:331–340, 1997
7. Le Lay S, Krief S, Farnier C, Lefrere I, Le Liepvre X, Bazin R, Ferre P, Dugail I: Cholesterol, a cell size-dependent signal that regulates glucose metabolism and gene expression in adipocytes. *J Biol Chem* 276:16904–16910, 2001
8. Warnock DE, Roberts C, Lutz MS, Blackburn WA, Young WW Jr, Baenziger JU: Determination of plasma membrane lipid mass and composition in cultured Chinese hamster ovary cells using high gradient magnetic affinity chromatography. *J Biol Chem* 268:10145–10153, 1993
9. Hao M, Lin SX, Karylowski OJ, Wustner D, McGraw TE, Maxfield FR: Vesicular and non-vesicular sterol transport in living cells: the endocytic recycling compartment is a major sterol storage organelle. *J Biol Chem* 277:609–617, 2002
10. Simons K, Ikonen E: Functional rafts in cell membranes. *Nature* 387:569–572, 1997
11. Brown DA, London E: Structure and function of sphingolipid- and cholesterol-rich membrane rafts. *J Biol Chem* 275:17221–17224, 2000
12. Xu X, London E: The effect of sterol structure on membrane lipid domains reveals how cholesterol can induce lipid domain formation. *Biochemistry* 39:843–849, 2000
13. Xia F, Gao X, Kwan E, Lam PP, Chan L, Sy K, Sheu L, Wheeler MB, Gaisano HY, Tsushima RG: Disruption of pancreatic beta-cell lipid rafts modifies Kv2.1 channel gating and insulin exocytosis. *J Biol Chem* 279:24685–24691, 2004
14. Takahashi N, Hatakeyama H, Okado H, Miwa A, Kishimoto T, Kojima T, Abe T, Kasai H: Sequential exocytosis of insulin granules is associated with redistribution of SNAP25. *J Cell Biol* 165:255–262, 2004
15. Veluthakal R, Chvyrkova I, Tannous M, McDonald P, Amin R, Hadden T, Thurmond DC, Quon MJ, Kowluru A: Essential role for membrane lipid rafts in interleukin-1β-induced nitric oxide release from insulin-secreting cells: potential regulation by caveolin-1+. *Diabetes* 54:2576–2585, 2005
16. Gruen ML, Saraswathi V, Nuotio-Antar AM, Plummer MR, Coenen KR, Hasty AH: Plasma insulin levels predict atherosclerotic lesion burden in obese hyperlipidemic mice. *Atherosclerosis* 186:54–64, 2006
17. Hao M, Li X, Rizzo MA, Rocheleau JV, Dawant BM, Piston DW: Regulation of two insulin granule populations within the reserve pool by distinct calcium sources. *J Cell Sci* 118:5873–5884, 2005
18. Hohmeier HE, Mulder H, Chen G, Henkel-Rieger R, Prentki M, Newgard CB: Isolation of INS-1-derived cell lines with robust ATP-sensitive K+ channel-dependent and -independent glucose-stimulated insulin secretion. *Diabetes* 49:424–430, 2000
19. Gunawardana SC, Rocheleau JV, Head WS, Piston DW: Mechanisms of time-dependent potentiation of insulin release: involvement of nitric oxide synthase. *Diabetes* 55:1029–1033, 2006
20. Mayor S, Sabharanjak S, Maxfield FR: Cholesterol-dependent retention of GPI-anchored proteins in endosomes. *Embo J* 17:4626–4638, 1998
21. Goward CR, Hartwell R, Atkinson T, Scawen MD: The purification and characterization of glucokinase from the thermophile Bacillus stearothermophilus. *Biochem J* 237:415–420, 1986
22. Rizzo MA, Magnuson MA, Drain PF, Piston DW: A functional link between glucokinase binding to insulin granules and conformational alterations in response to glucose and insulin. *J Biol Chem* 277:34168–34175, 2002
23. Vidal J, Verchere CB, Andrikopoulos S, Wang F, Hull RL, Cnop M, Olin KL, LeBoeuf RC, O'Brien KD, Chait A, Kahn SE: The effect of apolipoprotein E deficiency on islet amyloid deposition in human islet amyloid polypeptide transgenic mice. *Diabetologia* 46:71–79, 2003
24. D'Ambra R, Surana M, Efrat S, Starr RG, Fleischer N: Regulation of insulin secretion from beta-cell lines derived from transgenic mice insulinomas resembles that of normal beta-cells. *Endocrinology* 126:2815–2822, 1990
25. Gee KR, Zhou ZL, Qian WJ, Kennedy R: Detection and imaging of zinc secretion from pancreatic beta-cells using a new fluorescent zinc indicator. *J Am Chem Soc* 124:776–778, 2002
26. Bennett BD, Jetton TL, Ying G, Magnuson MA, Piston DW: Quantitative subcellular imaging of glucose metabolism within intact pancreatic islets. *J Biol Chem* 271:3647–3651, 1996
27. Postic C, Shiota M, Magnuson MA: Cell-specific roles of glucokinase in glucose homeostasis. *Recent Prog Horm Res* 56:195–217, 2001
28. Gloyn AL: Glucokinase (GCK) mutations in hyper- and hypoglycemia: maturity-onset diabetes of the young, permanent neonatal diabetes, and hyperinsulinemia of infancy. *Hum Mutat* 22:353–362, 2003
29. Rizzo MA, Piston DW: Regulation of beta cell glucokinase by S-nitrosylation and association with nitric oxide synthase. *J Cell Biol* 161:243–248, 2003
30. Yancey PG, Rodrigueza WV, Kilsdonk EP, Stoudt GW, Johnson WJ, Phillips MC, Rothblat GH: Cellular cholesterol efflux mediated by cyclodextrins. Demonstration Of kinetic pools and mechanism of efflux. *J Biol Chem* 271:16026–16034, 1996
31. Ort T, Maksimova E, Dirkx R, Kachinsky AM, Berghs S, Froehner SC, Solimena M: The receptor tyrosine phosphatase-like protein ICA512 binds the PDZ domains of beta2-syntrophin and nNOS in pancreatic beta-cells. *Eur J Cell Biol* 79:621–630, 2000
32. Ghosh DK, Abu-Soud HM, Stuehr DJ: Domains of macrophage N(O) synthase have divergent roles in forming and stabilizing the active dimeric enzyme. *Biochemistry* 35:1444–1449, 1996
33. Tzeng E, Billiar TR, Robbins PD, Loftus M, Stuehr DJ: Expression of human inducible nitric oxide synthase in a tetrahydrobiopterin (H4B)-deficient cell line: H4B promotes assembly of enzyme subunits into an active dimer. *Proc Natl Acad Sci U S A* 92:11771–11775, 1995
34. Klatt P, Schmidt K, Lehner D, Glatter O, Bachinger HP, Mayer B: Structural analysis of porcine brain nitric oxide synthase reveals a role for tetrahydrobiopterin and L-arginine in the formation of an SDS-resistant dimer. *Embo J* 14:3687–3695, 1995
35. Lajoix AD, Pugniere M, Roquet F, Mani JC, Dietz S, Linck N, Faurie F, Ribes G, Petit P, Gross R: Changes in the dimeric state of neuronal nitric oxide synthase affect the kinetics of secretagogue-induced insulin response. *Diabetes* 53:1467–1474, 2004
36. de Bont N, Netea MG, Demacker PN, Verschueren I, Kullberg BJ, van Dijk KW, van der Meer JW, Stalenhoef AF: Apolipoprotein E knock-out mice are highly susceptible to endotoxemia and Klebsiella pneumoniae infection. *J Lipid Res* 40:680–685, 1999
37. Roehrich ME, Mooser V, Lenain V, Herz J, Nimpf J, Azhar S, Bideau M, Capponi A, Nicod P, Haefliger JA, Waeber G: Insulin-secreting beta-cell dysfunction induced by human lipoproteins. *J Biol Chem* 278:18368–18375, 2003
38. Gao J, Katagiri H, Ishigaki Y, Yamada T, Ogihara T, Imai J, Uno K, Hasegawa Y, Kanzaki M, Yamamoto TT, Ishibashi S, Oka Y: Involvement of apolipoprotein E in excess fat accumulation and insulin resistance. *Diabetes* 56:24–33, 2007

Downloaded from http://diabetesjournals.org/diabetes/article-pdf/56/9/2328/388997/zdb00907002328.pdf by guest on 29 June 2022

39. Goldstein JL, Brown MS: Molecular medicine: the cholesterol quartet. *Science* 292:1310–1312, 2001
40. Simons K, Ehehalt R: Cholesterol, lipid rafts, and disease. *J Clin Invest* 110:597–603, 2002
41. Abulrob A, Tauskela JS, Mealing G, Brunette E, Faid K, Stanimirovic D: Protection by cholesterol-extracting cyclodextrins: a role for N-methyl-D-aspartate receptor redistribution. *J Neurochem* 92:1477–1486, 2005
42. Hao M, Mukherjee S, Sun Y, Maxfield FR: Effects of cholesterol depletion and increased lipid unsaturation on the properties of endocytic membranes. *J Biol Chem* 279:14171–14178, 2004
43. Dhanvantari S, Loh YP: Lipid raft association of carboxypeptidase E is necessary for its function as a regulated secretory pathway sorting receptor. *J Biol Chem* 275:29887–29893, 2000
44. Gondre-Lewis MC, Petrache HI, Wassif CA, Harries D, Parsegian A, Porter FD, Loh YP: Abnormal sterols in cholesterol-deficiency diseases cause secretory granule malformation and decreased membrane curvature. *J Cell Sci* 119:1876–1885, 2006
45. Arya R, Duggirala R, Almasy L, Rainwater DL, Mahaney MC, Cole S, Dyer TD, Williams K, Leach RJ, Hixson JE, MacCluer JW, O'Connell P, Stern MP, Blangero J: Linkage of high-density lipoprotein-cholesterol concentrations to a locus on chromosome 9p in Mexican Americans. *Nat Genet* 30:102–105, 2002
46. Freeman DJ, Norrie J, Sattar N, Neely RD, Cobbe SM, Ford I, Isles C, Lorimer AR, Macfarlane PW, McKillop JH, Packard CJ, Shepherd J, Gaw A: Pravastatin and the development of diabetes mellitus: evidence for a protective treatment effect in the West of Scotland Coronary Prevention Study. *Circulation* 103:357–362, 2001
47. Briones ER, Steiger DL, Palumbo PJ, O'Fallon WM, Langworthy AL, Zimmerman BR, Kottke BA: Sterol excretion and cholesterol absorption in diabetics and nondiabetics with and without hyperlipidemia. *Am J Clin Nutr* 44:353–361, 1986
48. Gylling H, Miettinen TA: Cholesterol absorption, synthesis, and LDL metabolism in NIDDM. *Diabetes Care* 20:90–95, 1997
49. Stranberg TE, Salomaa V, Vanhanen H, Miettinen TA: Associations of fasting blood glucose with cholesterol absorption and synthesis in nondiabetic middle-aged men. *Diabetes* 45:755–761, 1996
50. Sutherland WH, Scott RS, Lintott CJ, Robertson MC, Stapely SA, Cox C: Plasma non-cholesterol sterols in patients with non-insulin dependent diabetes mellitus. *Horm Metab Res* 24:172–175, 1992

Downloaded from http://diabetesjournals.org/diabetes/article-pdf/56/9/2328/388997/zdb00907002328.pdf by guest on 29 June 2022